

Positive Cloud-to-Ground Lightning Characteristics in the Eyewall of Typhoon Faxai (2019) Observed by Tokyo Lightning Mapping Array

Namiko SAKURAI

National Research Institute for Earth Science and Disaster Resilience (NIED), Tsukuba, Japan

Hironori FUDEYASU

Graduate School of Education, Yokohama National University, Yokohama, Japan

Typhoon Science and Technology Research Center, Yokohama National University, Yokohama, Japan

Paul R. KREHBIEL, Ronald J. THOMAS, William RISON, and Daniel RODEHEFFER

New Mexico Institute of Mining and Technology, New Mexico, USA

(Manuscript received 1 August 2021, in final form 25 August 2022)

Abstract

Although a number of studies have been conducted of the lightning activity in hurricanes and typhoons, little information has been obtained on the three-dimensional (3-D) structure of the lightning, or how it is related to the precipitation structures within the storms. Here, we utilize observational data from the 3-D Tokyo Lightning Mapping Array (Tokyo LMA), a Japan Meteorological Agency C-band Doppler radar, and the Japanese Lightning Detection Network (JLDN) to conduct a study of the lightning activity during Typhoon Faxai (2019) in comparison with the storm's precipitation structure. This is done for the dissipating stage of the typhoon, when the eyewall was well within the range of the instruments and undergoing a surge in lightning activity. Of particular interest in the surge was the occurrence of numerous positive cloud-to-ground (+CG) lightning flashes. Detailed study of the Tokyo LMA and JLDN data shows that, out of 52 flashes during the surge, 29 flashes or 56 % produced positive strokes to ground, an unheard of number considering that, from the lightning and 3-D radar structures, the storm appeared to be normally electrified, and under such circumstances would produce negative rather than positive strokes to ground. It also focuses attention on the question of how +CGs are produced in tropical cyclones in the first place. Based on a lack of -CG strokes and the LMA observations showing that the +CG strokes are produced mid-way or toward the end of normal polarity intracloud (IC) flashes, it appears that the dissipating storm cells have a depleted or horizontally sheared mid-level negative charge, such that an IC flash propagating into and through upper positive storm charge effectively funnels a steadily increasing amount of positive charge into the mid-level initiation region, eventually causing the positive breakdown of the IC flash to turn downward toward ground, producing a +CG stroke.

Keywords lightning; Lightning Mapping Array; typhoon; positive cloud-to-ground lightning

Corresponding author: Namiko Sakurai, National Research Institute for Earth Science and Disaster Resilience (NIED), 3-1, Tennodai, Tsukuba, Ibaraki 305-0006, Japan
E-mail: sakurain@bosai.go.jp
J-stage Advance Published Date: 15 September 2022

Citation Sakurai, N., H. Fudeyasu, P. R. Krehbiel, R. J. Thomas, W. Rison, and D. Rodeheffer, 2022: Positive cloud-to-ground lightning characteristics in the eyewall of Typhoon Faxai (2019) observed by Tokyo Lightning Mapping Array. *J. Meteor. Soc. Japan*, **100**, 979–993, doi:10.2151/jmsj.2022-051.

1. Introduction

Tropical cyclones (TCs) are one of the most destructive natural phenomena on Earth and are regularly related to the loss of life as well as extensive property damage. Lightning has been observed in many TCs (e.g., Black and Hallett 1999; Molinari et al. 1999; Nakano et al. 2011; Price et al. 2009). Price et al. (2009) found that an increase in lightning frequency in TCs preceded the intensification of their maximum sustained winds and minimum pressures approximately 1 day before the peak winds. They suggested that monitoring of lightning activity within a TC might be useful for predicting TC intensification.

Most lightning discharges in TCs have been observed in the eyewall and outer rainband, with relatively few being observed in the inner rainband (e.g., Molinari et al. 1999; Nakano et al. 2011; Yokoyama and Takayabu 2008). Zhang et al. (2012) reported that the radial distribution of the lightning varies with the intensity of TCs. They suggested that the lightning activity in TCs is closely related to the internal structure of their precipitation system. However, there are only a few observational reports on the relationship between the lightning activity and the three-dimensional (3-D) structure of precipitation systems in TCs. Squires and Businger (2008) reported case studies of the vertical structure of precipitation in the eyewall; there was deep convection in the eyewall region and enhanced reflectivities above the melting layer with a gradual decrease of reflectivity with height. Fierro et al. (2011) utilized observations of large-amplitude narrow bipolar events to study lightning in the eyewall of Hurricanes Rita and Katrina (2005) using the Los Alamos Sferic Array. The observations revealed a general increase in discharge heights during the rapid intensification period of convective elements in the eyewall.

A few studies have been conducted concerning the polarity of cloud-to-ground (CG) lightning in TCs. Samsury and Orville (1994) investigated the polarity of CGs in Hurricanes Hugo and Jerry (1989) and reported that more than 20 % of CGs were positive in both hurricanes. Similar results were reported by Zhang et al. (2012), who analyzed 18 typhoons. Thomas et al. (2010) investigated the polarity of CGs

in the eyewall of Hurricanes Emily, Katrina, and Rita (2005) using the World Wide Lightning Location Network and found that a high frequency of positive CGs occurred in the decaying stage of the hurricanes. If high frequencies of positive CGs occur commonly in the eyewall of the decaying stage of TCs, monitoring of positive CGs might be useful for predicting TC decay. Additional case studies or statistical analyses of the relationship between the TC phase and the occurrence of high percentage of positive CG in the eyewall would further help in the validation. Additionally, analysis of the internal structure of precipitation systems in the eyewall has been needed to clarify the mechanism by which the positive CGs are produced.

Typhoon Faxai (T1915) struck the Kanto region of Japan during September 8 and 9, 2019, producing many lightning discharges. 3-D observations of the total lightning activity in the typhoon were obtained using the Tokyo Lightning Mapping Array (Tokyo LMA), which has been set up and operated in the Tokyo metropolitan area by the National Research Institute for Earth Science and Disaster Resilience beginning in March 2017 (Sakurai et al. 2021). The objective of the present study is to describe the characteristics of the lightning activity in comparison with the internal structure of precipitation in the eyewall, using data from the Tokyo LMA, the Japan Meteorological Agency (JMA) C-band Doppler Radar (CDR), and the Japanese Lightning Detection Network (JLDN).

2. Data and method

2.1 Tokyo Lightning Mapping Array

The Tokyo LMA consists of 12 stations (Sakurai et al. 2021) (Fig. 1), 8 of which monitored the lightning during the typhoon. Each sensor detects the arrival time of impulsive very-high-frequency (VHF) radiation produced by electrical breakdown as the lightning propagates through a thunderstorm (Rison et al. 1999; Thomas et al. 2004). Peak events are detected in successive 80 μ s time windows for signals above a threshold value. The stations of the Tokyo LMA are distributed over a 90-km diameter area and can detect lightning activity as far as 200–300 km distance from the center of the network (Fig. 3b). The system typically locates tens to several hundred VHF

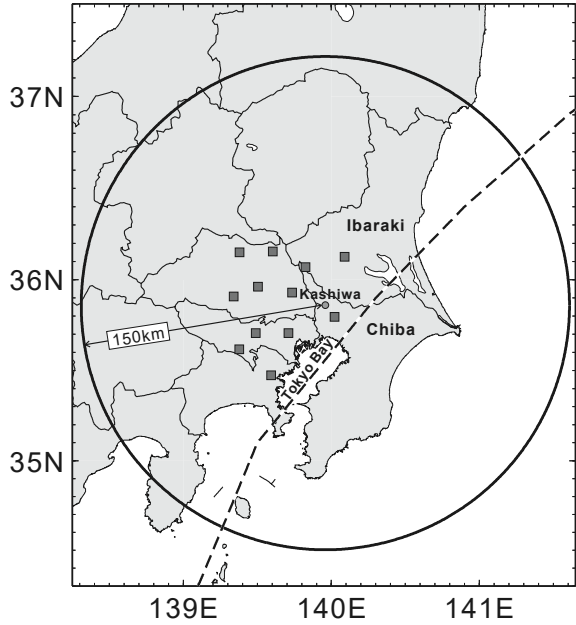


Fig. 1. Map depicting the locations of Tokyo LMA observation stations (square dots) and the JMA C-band Doppler Radar (CDR; circular dot). The circle indicates the coverage area of the JMA CDR and the scale of the map. The dashed line shows the path of T1915.

sources per flash, which reveals the development of individual flashes and helps in identifying their type.

2.2 JMA C-band Doppler radar

Data from the CDR were used to determine the internal structure of the precipitation systems in T1915. The radar was operated by JMA at the Kashiwa station and provided observations out to a radius of 150 km (Fig. 1). It scanned the typhoon in Plan Position Indicator scan mode with 26 elevation angles between 0° and 25° and measured the horizontal reflectivity Z_H , with a volume scan time of 10 min. The Z_H values were interpolated into a cartesian grid system (Cressman 1959) having a spatial resolution of 1 km horizontally and 250 m vertically.

2.3 Japanese Lightning Detection Network

The JLDN observations were used to investigate lightning ground strike locations and the peak currents of strokes. JLDN consists of 31 LF band sensors and provides coverage over all of Japan. The reported uncertainty of the JLDN locations is less than 500 m, and the minimum peak current of lightning discharges

detected by JLDN is approximately 3–5 kA (see <https://www.franklinjapan.jp/en/jldn/>).

3. Results

3.1 Overview

Figures 2 and 3 provide an overview of the lightning activity that occurred as the typhoon passed over the Kanto area, and how the activity was related to the typhoon's life cycle. T1915 developed from a tropical depression into a typhoon in the sea south of Minamitorishima at 0300 JST on September 5, 2019, and its central pressure decreased to 955 hPa at 0300 JST on September 8, 2019 (Figs. 2b, 3a). Simultaneously, the maximum wind speed around the center of the typhoon increased to 45 m s^{-1} . The typhoon began to decay at 0900 JST on September 9 (Fig. 2b) and subsided into an extratropical cyclone at 0900 JST on September 10.

Lightning started to be detected in the typhoon by the Tokyo LMA at 1524 JST on September 8 (initial burst of sources in Fig. 2a), while the typhoon was ~ 300 km south of the Tokyo LMA (southernmost dark blue sources in Fig. 3b). Figure 3c shows the typhoon's radar-observed precipitation structure at 1901 JST on September 8, along with the location of the lightning sources at that time (black "x" symbols in Fig. 3c and some of the light green sources in Fig. 3b). A close examination of Fig. 3c shows that the lightning was occurring primarily in the developing eyewall of the typhoon, with a lesser amount in an inner rainband. At this point, the typhoon was centered ~ 230 km south of the Tokyo LMA.

After a 4-hour quiescent period or "lull" in the LMA observations, the lightning activity started up again, this time primarily in the easternmost outer rainband (second burst of activity in Fig. 2a and orange sources in Fig. 3b). During this time (0200 JST–0500 JST on September 9), the typhoon had an axisymmetric eyewall structure (Fig. 3d) and propagated over Tokyo Bay and the Kanto region. Although a small amount of lightning occurred in the eyewall during this time, the main activity was in the eastern outer rainband. Four hours later, as the typhoon weakened and moved offshore east of Ibaraki Prefecture (Fig. 3e), a third burst of lightning occurred in the expanded eyewall structure (red sources in Fig. 3b and the final activity in Fig. 2a). As can be seen from Fig. 2b, the final lightning activity occurred as the typhoon transitioned from its mature stage to the decaying stage.

In summary, the observations show that the lightning was episodic in nature, with each episode lasting approximately 4 h (Fig. 2a) and occurring at different

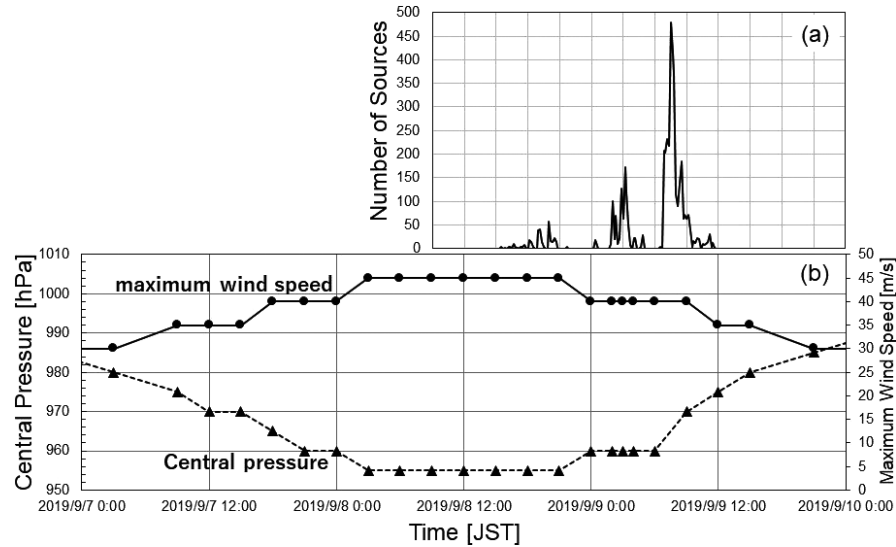


Fig. 2. a) Time series of the number of VHF lightning sources observed by Tokyo LMA from 0900 JST on September 8 to 0000 JST on September 10, 2019, illustrating the episodic nature of the lightning activity and the increase in detection efficiency as the typhoon approached the Tokyo LMA. b) Evolution of the central pressure and maximum wind speed of T1915 from 0000 JST on September 7 to 0000 JST on September 10, 2019, showing that the final episode of lightning occurred as the typhoon began its final decay.

stages in the typhoon's life cycle. A total of 7152 VHF sources were detected by 7 or more stations during the episodes, with the detection efficiency increasing as the typhoon approached and passed by the Tokyo LMA. There were fewer lightning sources in the inner rainband than in the eyewall or the outer rainband, in agreement with the radial distribution of lightning activity in TCs reported by earlier studies (e.g., Molinari et al. 1999; Nakano et al. 2011; Yokoyama and Takayabu 2008).

3.2 Lightning observations

Figure 4 shows an overview of the total lightning activity during the final, decaying stage of the typhoon, as determined by the Tokyo LMA and the JLDN. The Tokyo LMA observations are colored both as a function of time (Fig. 4a) and by the logarithmic density of sources (Fig. 4b). A total of 55 flashes occurred between 0643 and 0858 JST (2:15 h) on September 9, corresponding to an hourly flash rate of $\sim 24 \text{ h}^{-1}$. During this time, the JLDN detected 52 of the flashes, with 36 of the flashes reported as being CG discharges and 16 reported as being intracloud (IC) flashes. The total number of JLDN sferic events was 278, corresponding to an average of ~ 5 events per flash. Of the 36 CGs, 32 were reported by the JLDN

as being +CG flashes, and 4 were reported as -CGs. Comparing the JLDN events on a flash-by-flash basis with the more detailed observations by the Tokyo LMA (e.g., Fig. 6) shows that in actuality there were 29 +CG flashes and only 1 -CG flash, with 3 of the JLDN-indicated +CG flashes and 3 of the -CG flashes being misidentified as IC flashes (Table 1). Thus, 29/52 or 56 % of the total number of flashes were +CGs, with the +CGs being approximately 1.3 times more than IC flashes.

The JLDN-detected sferic events are presented in histogram form in Fig. 5. Sferic counts for positive and negative CG events are shown in the upper right and left quadrants, respectively, as a function of their peak currents. IC events of positive and negative polarity are shown in the lower quadrants and occur in much larger numbers, as indicated by the different vertical scales. Overall, the histograms graphically illustrate the dominance of +CG events in the eyewall of the decaying stage of the typhoon and the wide range of their peak currents (~ 30 –130 kA). Events having peak currents less than +20 kA are known as “weak positive” events (in pink) and are misidentified +IC events, as evidenced by their incidence rate versus peak current being the same as that of the +IC events, and constituting a small fraction of the much larger

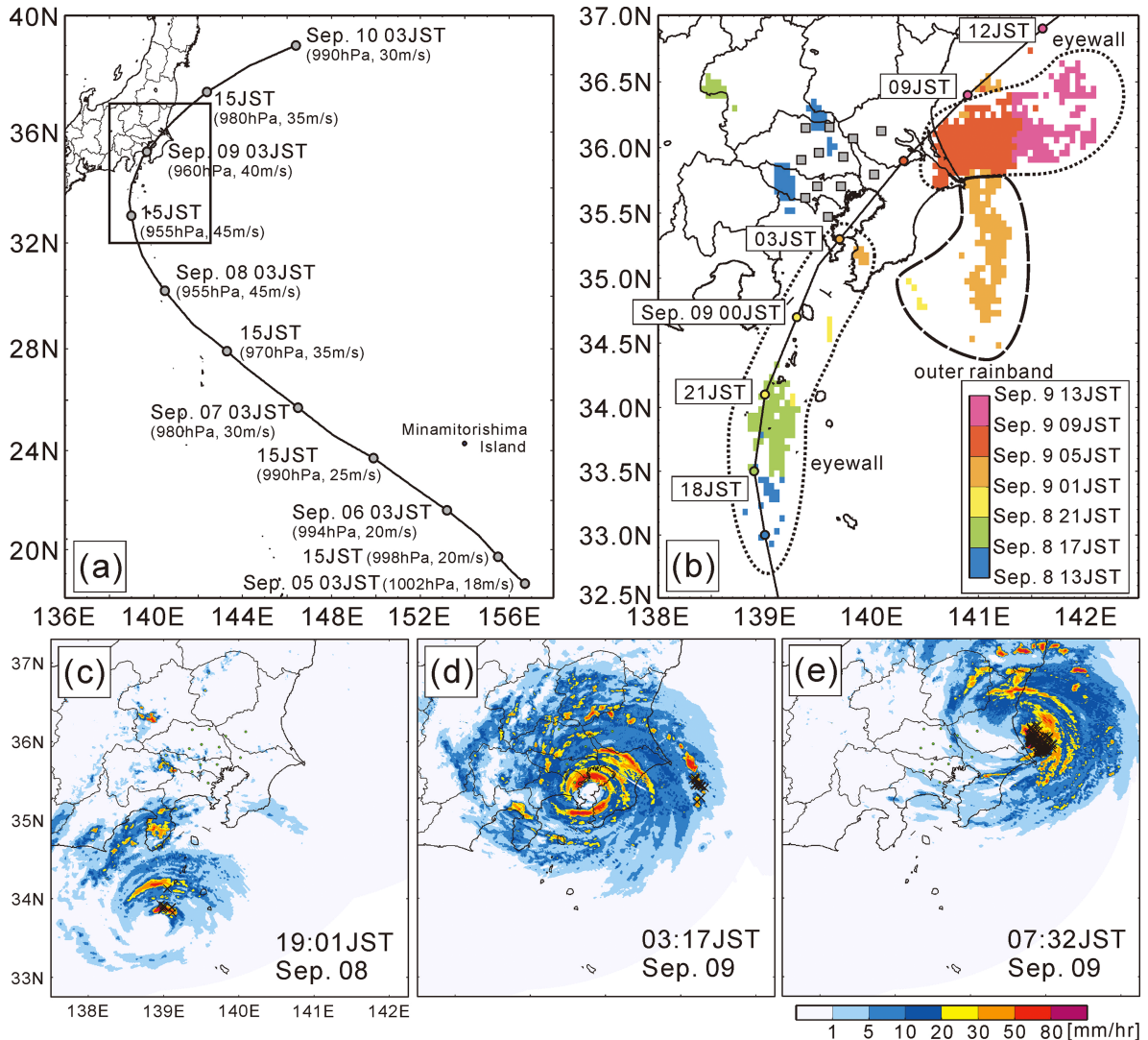


Fig. 3. a) Trajectory of T1915 over the 5-day time period of its overall development. b) Zoomed in view of the lightning activity as the typhoon approached and passed by the Tokyo LMA. (c–e) Radar observations of the typhoon's structure and the lightning activity ("x" marks) around the time of (c) initial lightning detection by the Tokyo LMA (dark blue and light green eyewall sources in b), (d) as the eyewall of T1915 moved over Tokyo Bay (yellow and orange outer rainband sources in b), and e) during the decaying stage showing its dense and widespread lightning activity (red sources in b). Rainfall intensity near the ground was observed by eXtended Radar Information Network (XRAIN) operated by Japan's Ministry of Land, Infrastructure, Transport and Tourism. Dark blue sources near the Tokyo LMA stations are unrelated local lightning activity prior to the approaching typhoon.

number of +ICs. It is well known that weak positive events are misidentified +IC events produced by normal polarity IC flashes, due to their sferics being similar and difficult to distinguish between (Cummins et al. 1998; Cummins and Murphy 2009).

Similarly considered to be in the IC category are the

relatively weak -CG events (light blue, Fig. 5). This is determined in part by their peak currents being weak (less than 10 kA) and/or by the LMA observations showing that the events occurred within the first millisecond or so of the flashes, with insufficient time for a downward negative leader to propagate to ground. (An

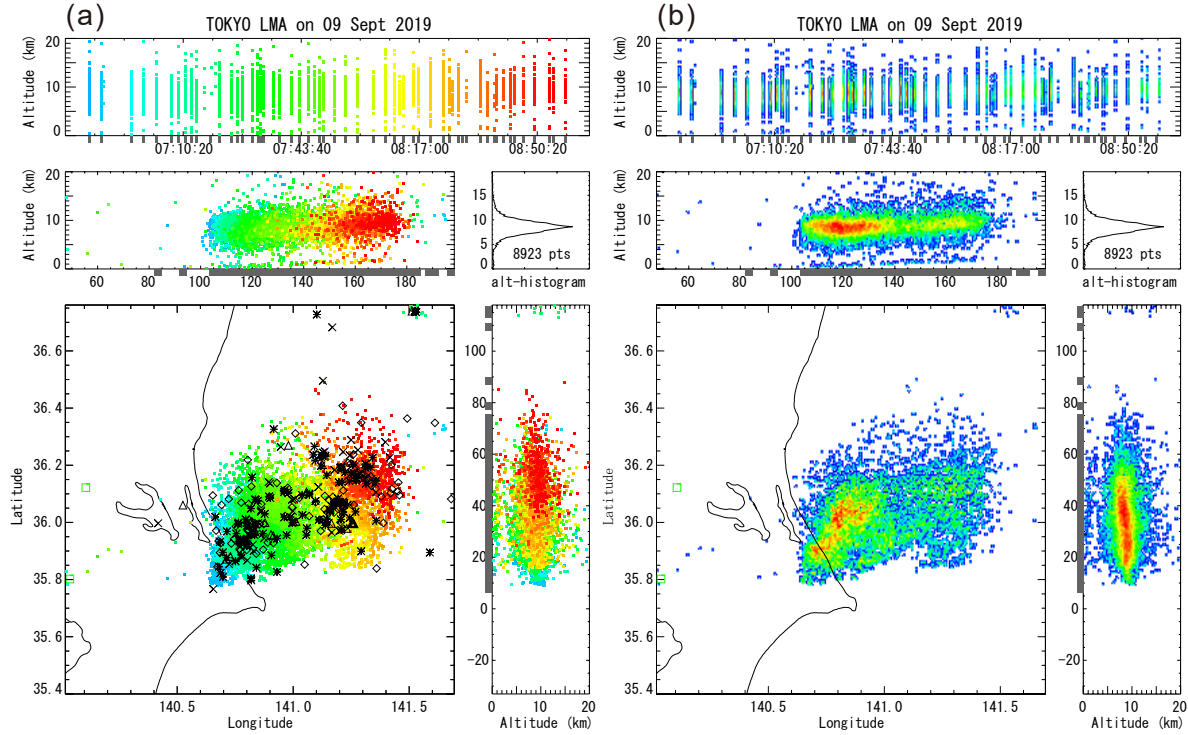


Fig. 4. Overview of the lightning activity in the eyewall of the decaying stage of T1915, as determined by the Tokyo LMA. Fifty-five lightning flashes occurred over a 2-h and 15-min time period. a) Temporal progression of the VHF sources. b) Logarithmic density of the sources. Triangle, cross, diamond, and star marks in the plan views indicate the location of $-CG$, $+CG$, $-IC$, and $+IC$ events detected by JLDN, respectively (shown as gray bars at the base of the vertical projection panels). Square green symbols at the left edge of the plan panels indicate two easternmost Tokyo LMA stations. (Plots utilize solutions from six or more stations).

Table 1. The number of flashes observed in the eyewall between 0643 JST and 0858 JST on September 9. a) The number of flashes detected by both the Tokyo LMA and the JLDN. b) The number of IC and CG flashes determined by JLDN. c) The number of CG flashes of each polarity determined by JLDN. d) The number of flashes as determined utilizing the Tokyo LMA data (see text). e) The corrected total number of IC and CG flashes.

All flashes							
52							
IC	CG						
16	36						
	$-CG$		$+CG$		$\pm CG$		
	4		23		9		
	$-CG$	IC	$+CG$	IC	$+CG$	$-CG$	IC
	1	3	21	2	8	0	1
22	1		29		0		

example of an incorrectly identified weak negative CG event is seen at the beginning of the example flash of Fig. 6, where it is also substantially mislocated.) Instead, there was only 1 actual $-CG$ flash (the 37th flash at 08:16:49 JST in Fig. 4). The flash produced multiple strokes to ground, and the second was doubly detected as a 38/39-kA $-CG$ stroke. From the LMA observations, and as discussed further below, the $-CG$ flash was immediately preceded by a strong, doubly detected $+CG$ flash, which would have diminished the storm's positive charge, possibly allowing (or causing) the next flash to be a $-CG$. The dearth of $-CG$ flashes in the eyewall of the decaying stage of the typhoon is additionally indicated by the lack of LMA sources that are produced between the IC flashes and ground. That downward leaders of $-CG$ strokes are readily detected by the Tokyo LMA has been documented in the study of lightning by Sakurai et al. (2021).

It should be noted that six of the high-peak current

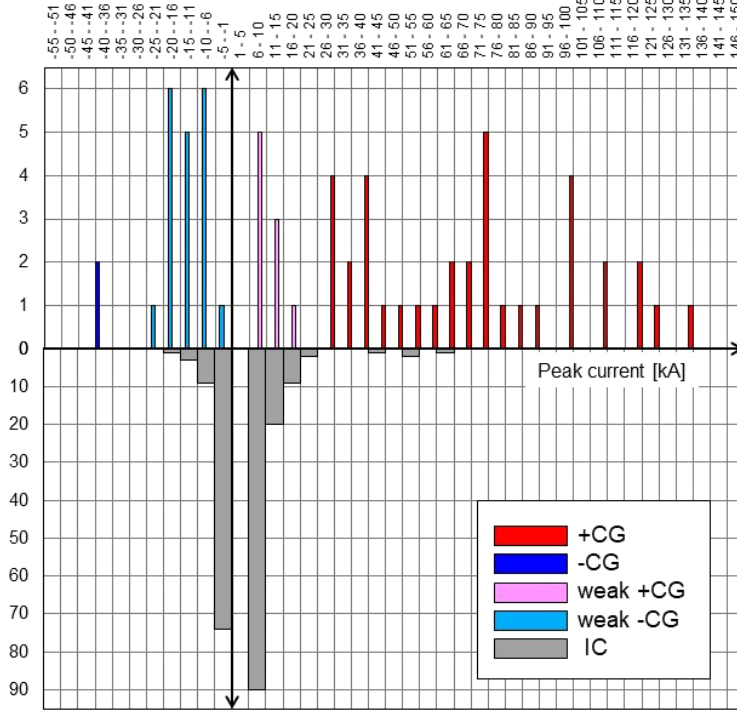


Fig. 5. Histograms of JLDN-detected sferic events versus peak current in the eyewall of the decaying stage of T1915. Sferics identified as CG events are shown in the upward histograms, with positive events on the right and negative events on the left. Much more numerous IC events are shown in the downward filled gray bars (note vertical scale difference).

+CG counts in Fig. 5 were doubly detected +CG strokes. Such doubly detected events occur within a few microseconds of each other and are readily recognized as corresponding to a single stroke. The double detections are caused by the strong sferic of the +CG stroke being located by two independent sets of JLDN stations and are often seen in the U.S. National Lightning Detection Network (NLDN) data. However, they are readily identified and affect only the stroke/event counts, but not the number of flashes. Finally, if the weak -CG events in the JLDN data were taken at face value, 8 out of the 29 +CG flashes would have included a negative ground stroke, making them appear to be hybrid +CG/-CG flashes (Table 1). Thus, determining flash statistics from sferics data alone would be misleading for understanding the typhoon lightning. At the same time, the VHF LMA observations alone would not have been able to distinguish between IC and CG events in the storm.

The combination of the LMA and JLDN shows that the positive strokes typically occurred partway through the flashes. Their occurrence was further confirmed

by characteristic reinvigoration or “blooming” of the LMA activity radially away from the extremities of branches in different directions around the plan location of the positive stroke. Figure 6 shows an example of such blooming following a 117-kA +CG stroke. This was the third flash in the decaying sequence of Fig. 4 and occurred at 06:55:38 JST on September 9. As with all the flashes in the decaying system, the 06:55:38 flash was a normal polarity IC discharge, beginning with upward negative breakdown into and horizontally through upper positive charge in the storm. The JLDN located three events within the first millisecond of the flash, the first and third of which were 17 kA and 14 kA +IC events, respectively, with their positive polarity consistent with being produced by upward negative breakdown. The second event was classified as a 14-kA -CG stroke, but is an example of a misclassified -CG. This is indicated by occurring at the very beginning of the flash, too early for a downward leader to reach ground and, in this case, being substantially mislocated, ~30 km to the NW of the other activity during the flash (black triangle in the

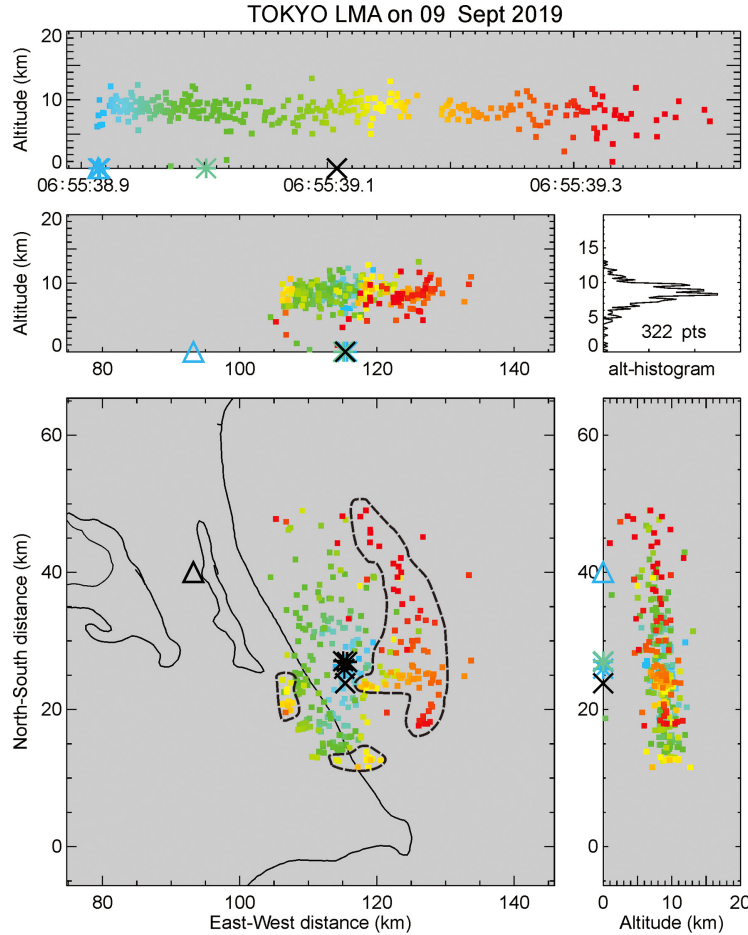


Fig. 6. VHF lightning sources for a +CG flash at 06:55:38 JST on September 9 that produced a 117-kA +CG discharge 200 ms into the flash (black X symbol). Arrival of ground potential within the cloud initiated characteristic “blooming” of the breakdown in different directions away from the extremities of the preceding activity, including an entirely new branch to the east and north (dashed areas). Triangle, cross, and star marks indicate the location and time of -CG, +CG, and +IC events detected by JLDN, respectively. (Plot shows sources located by six or more stations with chi-square values ≤ 5).

plan view of Fig. 6). The ensuing +CG stroke occurred approximately 200 ms into the flash (black X marker in each of the panels) and was correctly located by the JLDN. Significantly, and as will be discussed in more detail later, the +CG strike point was in close proximity to the plan flash initiation region. The post-stroke blooming is outlined by dashed areas in the plan view, which contain the yellow-orange-red sources following the positive stroke in the height-time panel. The blooming is caused by ground potential being introduced into the storm by the energetic return stroke of +CG flashes, which substantially reinvigorates the breakdown, extending the channels in space and time.

In this case, a new and extensive branch was initiated close to the flash initiation point that developed over a large area to the east and north.

Finally, an interesting feature of the observations concerns the lone -CG flash which, as discussed above, occurred at 08:16:49 JST as the 37th flash in the storm. In particular, the flash occurred one-half second after and in the exact same location and altitude as flash 36, which produced a strong, doubly detected 32/26 kA +CG stroke to ground. This preceding stroke would have deposited negative charge in the storm’s upper positive charge region which, combined with any other negative charge, might have caused or

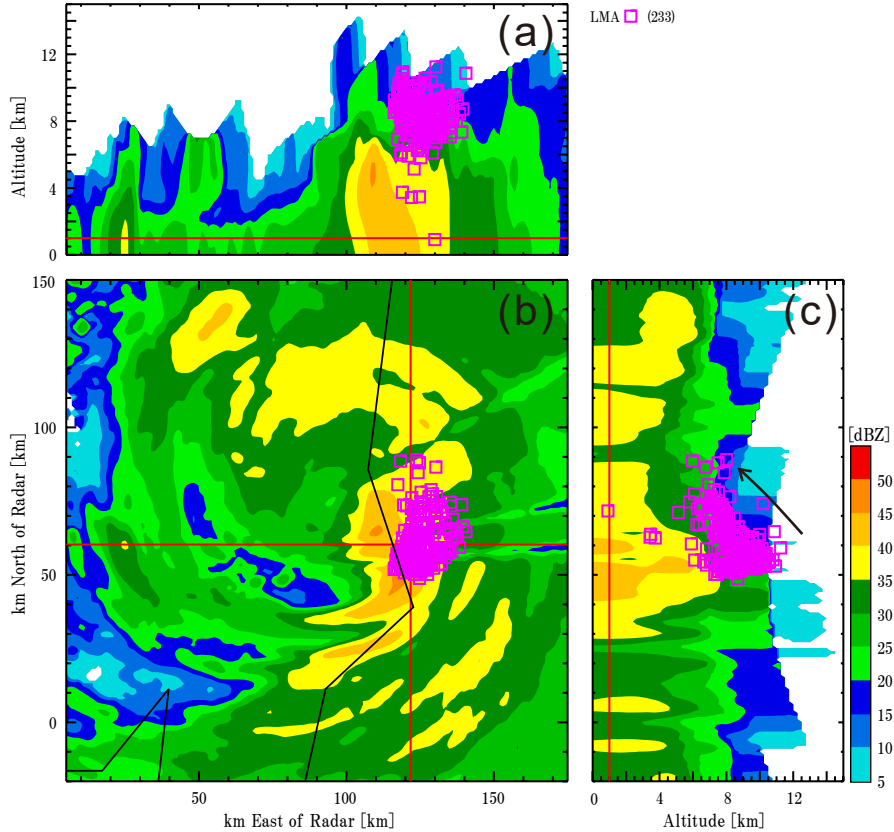


Fig. 7. Horizontal cross-section of the radar reflectivity at 1 km altitude (b) and east–west and north–south vertical cross-sections (a, c) at 0710 JST on September 9, 2019. Overlaid on the cross-sections are the VHF sources (□) for three horizontally extensive (20–25 km) lightning flashes between 0700 and 0710 JST. The VHF sources were produced by negative breakdown propagating through upper positive charge, which formed immediately above the convective core and was advected northward and eastward by the eyewall winds, descending somewhat in altitude away from the core (black arrow in c). Downward descent rate of the arrow is overly steep due to the vertical scale being greatly exaggerated relative to the horizontal scale (see Fig. 9).

assisted in the 37th flash being a $-CG$. Four minutes later, flash 38 occurred, again in the same location as the two previous flashes. This was a long-lasting ~ 600 ms duration flash that produced a prolific number (12) of weak positive and negative IC events, in the middle of which a single, high current ($+63$ kA) event occurred. Instead of being classified as a $+CG$, it was classified as a $+IC$ event. It is seen in the bottom right quadrant of the histogram plot of Fig. 5, but almost certainly a misclassified $+CG$ whose sferic waveform may have been made more complex by the unusual preceding activity. In any case, the complexity of the overall three-flash sequence is indicative of the substantial effect of lightning charge deposition altering the electrical charge structure and lightning

activity in storms (e.g., Coleman et al. 2003; Brothers et al. 2018).

3.3 Comparison with radar observations

The internal structure of precipitation systems in the eyewall of T1915 was investigated using the JMA CDR installed at Kashiwa (Fig. 1). Figure 7 shows how the lightning activity was related to the radar-derived reflectivity and precipitation structure during a 10-min time interval between 0700 JST and 0710 JST on September 9. The comparison shows that the lightning was occurring on the eastern side of the partial eyewall structure, where 30 dBZ reflectivity extended up to approximately 10 km altitude (Figs. 7a, c). Thirty-five dBZ reflectivity extended up to approx-

imately 7 km altitude in the convective core, which implies that not only ice crystals and super-cooled droplets but also graupel existed in the deep convection. Three lightning flashes occurred during the 10-min time interval, in particular the fifth, sixth, and seventh flashes of the overview plots of Fig. 4. In each case, the flashes began by discharging upper positive charge at $\sim 8\text{--}10$ km altitude above the convective core, where the reflectivity was between 30 and 20 dBZ, then progressed northward and downward to between ~ 6 km and 8 km altitude (black arrow in Fig. 7c), following the 30–20 dBZ contours. Similar downward development was observed during the flash of Fig. 6, which occurred in the same location ~ 4 min before the three-flash eyewall sequence. The altitude descent with northward propagation is consistent with the upper positive charge being advected northward by the typhoon's counterclockwise rotation and downward by the 20–30 dBZ contours decreasing in altitude off to the side of the core. In this altitude and reflectivity regime, the temperature would have been -30°C , and the hydrometeors would have consisted of crystalline ice particles and frozen cloud droplets, which are the carrier of upper positive charge in electrified storms.

To investigate the relationship between the vertical development of the precipitation and the lightning activity, a statistical analysis was conducted of the correlation between the 30 dBZ echo top height and the lightning activity versus time and location. The analysis period was the duration in which the center of T1915 was within range of the CDR (Fig. 1), and the analysis area was within 100 km of the typhoon's center. The Critical Success Index (CSI) of a positive correlation between 30 dBZ echo top height and the occurrence of lightning detected by the Tokyo LMA was 0.63 when echo top height of 30 dBZ exceeded 11 km. In addition, the CSI was 0.46 (0.59) when the height of 30 dBZ exceeded 9 km (10 km). Overall, the results support the premise that lightning developed in convective cells where ice crystals, graupel, and super-cooled cloud droplets were present to produce electrification by the non-inductive graupel–ice mechanism (Takahashi 1978).

3.4 Flash extents

The spatial extent of the VHF lightning sources can be regarded as a proxy of the extent of the charge region in storms having low flashing rates, since the flashes tend to propagate through the full extent of the charge regions. Figure 8 shows the distribution of flash extents in the eyewall from 0000 JST to 0900 JST on

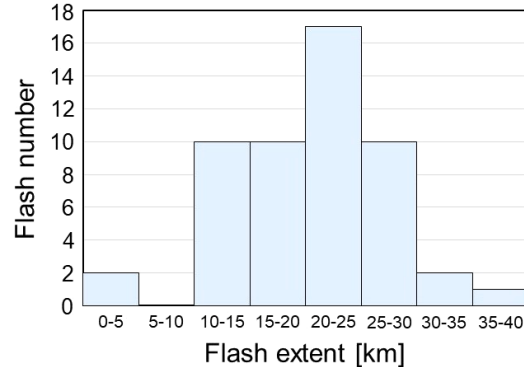


Fig. 8. Distribution of horizontal flash extents in the eyewall of T1915 between 0000 JST and 0900 JST on September 9, 2019.

September 9 when the typhoon center passed over Tokyo Bay, the north part of Chiba, Ibaraki Prefecture, and offshore of the Ibaraki Prefecture coast. The flash extent is defined as the square root of the horizontal convex hull (polygon) of the source locations, which in this study is the longitude–latitude plane. The definition is the same as the flash extent in previous studies (Bruning and MacGorman 2013; Mecikalski et al. 2015; Yoshida et al. 2019). In the present case, the analysis was applied to 50 of the lightning flashes in the decaying system between 0600 JST and 0900 JST and to two small lightning flashes that occurred in the eyewall as the center of the typhoon was passing near Tokyo Bay between 0000 JST and 0200 JST. The arithmetic mean of the flash extents was 20.6 km, the geometric mean was 19.3 km, and the median extent was 21.1 km. The maximum flash extent was 36.3 km, and the minimum extent was 4.8 km. The latter value corresponded to that of the two early flashes, both of which had extents less than 5 km. Otherwise, the minimum flash extents in the decaying sequence were typically $\sim 10\text{--}15$ km.

Table 2 compares the flash extents of the present study with those obtained by other investigators and storm types in Japan. Yoshida et al. (2019) investigated flash extents for lightning in the summer and winter seasons in Japan, which were observed by the Broadband Observation network for Lightning and Thunderstorms. They reported arithmetic mean and median flash extents of 6.5 km and 5.1 km in the summer season and 16.9 km and 14.8 km for winter storms. Zheng et al. (2019), using LMA observations of winter storms, reported arithmetic mean and median flash extents of 19.8 km and 18.3 km. Bruning

Table 2. Comparison of flash extents for four different storm types.

	T1915	Yoshida et al. (2018)		Zheng et al. (2019)
	typhoon FAXAI	summer lightning	winter lightning	winter lightning
arithmetic mean	20.6 km	6.5 km	16.9 km	19.8 km
median	21.1 km	5.1 km	14.8 km	18.3 km

and MacGorman (2013), using LMA observations of large Great Plains storms in the central U.S., reported flash widths/extents up to 20–30 km. The basic conclusion is that the flash extents depend on the size of the storms.

4. Discussion and conclusions

4.1 Storm charge structure and the cause of +CGs

From the radar and lightning comparisons of Fig. 7, the storm cells appear to have been normally electrified, with IC flashes occurring between mid-level negative and upper positive storm charges, produced by the standard non-inductive graupel–ice electification mechanism. This is supported by the VHF sources indicating upward negative development at the very beginning of the flashes, followed by horizontal propagation through upper positive charge. However, there is no evidence of opposite polarity positive breakdown propagating bidirectionally into and through mid-level negative charge, as is usually seen during normal polarity IC flashes, albeit on a weaker and delayed basis. In addition, storms having a normal polarity electrical structure invariably produce negative CG discharges (e.g., Krehbiel 1986; MacGorman and Rust 1998), for which the downward negative leaders to ground are readily detected at VHF (e.g., Shao et al. 1995; Sakurai et al. 2021). Instead, negative CG strokes were conspicuously absent, replaced instead by a large percentage of positive strokes to ground. This is unheard of in normally electrified storms in their convective stage of development. Such lightning activity is not explained by the storms being anomalously electrified, as in Great Plains storms studied during the Severe Thunderstorm Electrification and Precipitation Study (STEPS 2000; Lang et al. 2004a). In such storms, the +CG flashes are infrequent and vastly outnumbered by IC flashes, with the IC flashes being inverted in polarity between mid-level positive and upper-level negative charges (e.g., MacGorman et al. 2005). And not necessarily by winter storms, whose +CG discharges originate in horizontally distributed separate layers of positive and negative charges, at relatively low altitudes above sea level (e.g., Wang et al. 2021; Wu et al. 2021).

Figure 9 shows the lightning-inferred charge structure during a 15-min time interval at the beginning of the decaying stage of T1915, when the lightning was closest to the Tokyo LMA. Seven flashes occurred during the time interval, beginning with the example flash of Fig. 6 and including the three flashes used for the radar comparsion in Fig. 7. Unlike the radar overlay, where the exaggerated vertical scale makes the lightning sources appear to be compressed horizontally and expanded vertically, the sources in the vertical projections of Fig. 9 are plotted with a 1:1 aspect ratio, showing that in actuality they were highly layered vertically and horizontally extensive. The red sources correspond to negative breakdown propagating through upper positive charge. (The scattered additional sources are the same, but are slightly mislocated in altitude.) Consistent with the flash extent determinations, the flashes developed over areal extents up to ~40 km north to south and ~20 km east to west. The large extents are indicative of northward and eastward advection of the upper positive charge away from the convective core, as seen in the plan view of Fig. 7. Unusually, no sources could be identified as being due to positive breakdown through mid-level negative charge.

To help understand how the positive strokes to ground occur, it is instructive to look at how other types of +CG discharges are produced. Particularly useful in this regard are high-peak current +CG strokes that occur in the trailing stratiform regions of large mesoscale convective systems (MCCs), which are sufficiently energetic to produce luminous sprites in the upper atmosphere. From lightning charge center studies of similar, horizontally extensive stratiform discharges in Florida, energetic +CGs were found to occur as a result of negative breakdown propagating through positive charge just above the radar-detected bright band at the 0°C melting level (Krehbiel 1981; Section 3.3). The continuously propagating breakdown was shown to effectively transfer positive charge back to the opposite end of the conducting leader channels, where it built up to the point of eventually initiating a downward positive leader to ground and a +CG stroke. That the same mechanism produces +CG discharges

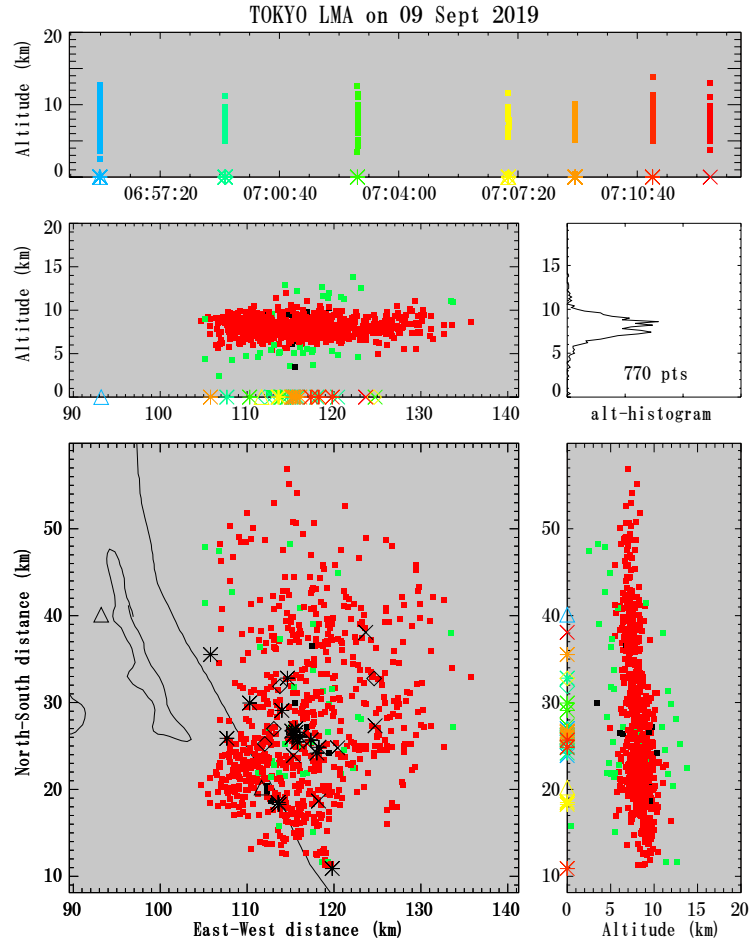


Fig. 9. LMA-inferred distribution of upper positive charge (red sources) corresponding to seven flashes at the beginning of the decaying stage of T1915, showing the layered nature and large horizontal extent of the charge caused by downwind advection away from the convective core. Black dots show the flash initiation locations above the core. Scattered green sources are slightly mislocated events. (Sources are six or more station solutions with chi-square ≤ 1 .)

in trailing stratiform regions of MCCs is readily seen in LMA observations of trailing stratiform lightning, such as those studied during STEPS 2000 (Lang et al. 2004b). In particular, NLDN-detected high-peak current +CG strokes are found to occur several kilometers behind the leading edge of the flash's negative breakdown, often at successive times and locations as the negative breakdown continues propagating.

In the context of the present study, rather than propagating through positive charge above a low-altitude radar bright band, as in stratiform situations, the negative breakdown of the IC flashes propagates through upper positive storm charge. However, similar to the lower altitude stratiform discharges, the negative

breakdown would be transferring an increasing amount of positive charge back into the flash initiation region. Normally, the positive charge would be deposited within the storm's mid-level negative charge by means of bidirectional positive leader activity. However, if the negative charge were to be depleted or displaced in comparison to the upper positive (e.g., by vertical wind shear), the accumulated or excess positive charge would end up producing a positive leader to ground, as in the stratiform +CG discharges. Evidence that this is how the +CG strokes are produced in the typhoon flashes is provided by the +CG strokes occurring relatively late in the flash's development (approximately half to 2/3 of the way through

the flash), providing time for positive charge to build up in the flash start region and producing a positive leader to ground. The resulting return stroke introduces ground potential into the storm, reinvigorating and extending the flash development and overall duration, as seen in the blooming of Fig. 6. Not all IC flashes would necessarily reach this threshold, but apparently a large fraction reach this threshold (29/52 or 56 % of the flashes in the present study). The strength of the resulting +CG stroke would be variable from one flash to the next, as seen in the broad range of peak currents for different flashes in Fig. 5. The resulting positive strokes are highly energetic, as evidenced by their peak currents and a notable fraction being doubly detected by the JLDN. Another indication of the mechanism is that when a positive stroke does occur, its JLDN ground strike location is relatively close to the plan location of flash initiation – i.e., where the negative breakdown started and where the positive charge would tend to be accumulated. This is seen, for example, in Fig. 6, where the JLDN source for the +CG stroke in the plan view panel is near the location of the flash's initial sources. In the Fig. 6 case, the post-stroke breakdown propagated in multiple directions away from its center initiation point. Even more striking are flashes where the breakdown propagated unidirectionally away from its initiation point, yet the +CG stroke is back at the starting point. An example of this was the 35th flash at 08:15:24 JST on September 9 (not shown), which developed 10 km unidirectionally away from its initiation point, then produced a doubly detected 116 kA +CG stroke back at and directly below the starting point, causing the flash to extend its unidirectional breakdown for an additional 10 km.

A possible cause for the main negative storm charge appearing to be depleted is the negative and upper positive charges being partially displaced horizontally from each other by vertical wind shear. Evidence that vertical shear has an effect on lightning in typhoons has been reported by Corbosiero and Molinari (2002). Also, Levin et al. (1996) showed that a good correlation existed between the fraction of positive CG flashes and wind shear in other types of thunderstorms.

4.2 Range of +CG peak currents

Another issue that is raised in the typhoon observations concerns the peak current values above which sferics identified as +CG events are actual strokes to ground, and below which they are weak positive events that are misidentified +IC sferics. Using blooming as an indicator of an actual stroke to ground,

and benefiting from the fortuitous occurrence of a relatively large number of +CGs, the peak transition current appears to be approximately 25 kA. A related question is whether non-return stroke IC events can occur at or above the transition value. The rapid decrease in the numbers of both positive and negative ICs at magnitudes above 15 kA in Fig. 5 indicates that IC peak currents above 25 kA are rare. Four such events were identified to occur in the JLDN data: flash 7 at 07:08:55 JST (a +51-kA event), flash 13 at 07:25:35 JST (a +42-kA event), flash 25 at 07:48:44 JST (a +51-kA event), and flash 38 at 08:20:11 JST (a +63-kA event) on September 9, all of which were classified as +ICs. However, due to producing strong blooming like that of +CGs of similar current magnitude, they were almost certainly misidentified +CGs, supporting the idea that high-peak current IC events (comparable to return stroke currents) do not occur.

4.3 Summary

The results of this study provide the first good understanding of eyewall lightning over a large area in the decaying phase of a typhoon, obtained from joint observations provided by the Tokyo LMA, the JLDN lightning detection network, and the Tokyo-based CDR of the JMA. The storm was highly unusual in that it produced a high percentage of +CG flashes, despite appearing to be normally electrified. The results are summarized as follows:

- Even in the decaying stage of the typhoon, the storms were strongly convective and normally electrified, in the same manner as other convective storms, namely by the non-inductive graupel–ice mechanism.
- That the otherwise normally electrified storm produced positive instead of negative CG flashes indicates that the convective core of the storm had a depleted mid-level negative charge.
- A possible explanation for the depletion is the negative and upper positive charges being displaced horizontally from each other by vertical wind shear.
- The storm's upper positive charge was advected downwind from above the convective core by strong upper-level winds, giving rise to horizontally extensive (up to 30–40 km) flash extents.
- The relative lack of mid-level negative charge resulted in individual IC flashes appearing to produce an increasing amount of positive charge back in the flash initiation region during the flash development, eventually causing positive breakdown downward to ground and producing the +CG strokes.
- The high percentage of energetic +CG strokes to

ground can be explained by the flashes all being IC-like, with every flash having a chance of continuing to ground (29/52 or 56 % in the present study).

- The resulting +CGs have a wide range of peak currents due to the positive charge accumulation changing from flash to flash, and not occurring in all flashes.
- The above explanation is the same basic process that produces sprite-producing +CG discharges in the trailing stratiform region of mesoscale convective complexes.
- A similar explanation may be applicable to +CG flashes in winter storms, whose +CG discharges originate in horizontally extensive regions of positive charge at relatively low altitudes above mean sea level.
- The peak current value above and below which actual +CGs and misclassified weak +CG events occur appears to be in the 20–25 kA range.

Data Availability Statement

The XRAIN data are available for download from DIAS at <https://diasjp.net/service/xrain-data/>. The JLDN data are not publicly available due to the management policy of Franklin Japan Co. Ltd. The other datasets generated and/or analyzed in this study are available from the corresponding author on reasonable usage upon request.

Acknowledgments

The authors are grateful to the editor and two anonymous reviewers for their comments that valuably improved the paper. We also thank the Innovation Hub Construction Support Project of the Japan Science and Technology Agency (JST) for supporting the acquisition of the Tokyo LMA. We are grateful to Dr. Kyle C. Wiens for supporting in the analysis using radar data and LMA data. The eXtended Radar Information Network (XRAIN) data sets used for this study are provided by the Ministry of Land, Infrastructure, Transport and Tourism, Japan. This dataset was also collected and provided under the Data Integration and Analysis System (DIAS), which was developed and operated by a project supported by the Ministry of Education, Culture, Sports, Science and Technology.

References

Black, R. A., and J. Hallett, 1999: Electrification of the hurricane. *J. Atmos. Sci.*, **56**, 2004–2028.

Brothers, M. D., E. C. Bruning, and E. R. Mansell, 2018: Investigating the relative contributions of charge deposition and turbulence in organizing charge within a thunderstorm. *J. Atmos. Sci.*, **75**, 3265–3284.

Bruning, E. C., and D. R. MacGorman, 2013: Theory and observations of controls on lightning flash size spectra. *J. Atmos. Sci.*, **70**, 4012–4029.

Coleman, L. M., T. C. Marshall, M. Stolzenburg, T. Hamlin, P. R. Krehbiel, W. Rison, and R. J. Thomas, 2003: Effects of charge and electrostatic potential on lightning propagation. *J. Geophys. Res.*, **108**, 4298, doi: 10.1029/2002JD002718.

Corbosiero, K. L., and J. Molinari, 2002: The effects of vertical wind shear on the distribution of convection in tropical cyclones. *Mon. Wea. Rev.*, **130**, 2110–2123.

Cressman, G. P., 1959: An operational objective analysis system. *Mon. Wea. Rev.*, **87**, 367–374.

Cummins, K. L., M. J. Murphy, E. A. Bardo, W. L. Hiscox, R. B. Pyle, and A. E. Pifer, 1998: A combined TOA/MDF technology upgrade of the U.S. National Lightning Detection Network. *J. Geophys. Res.*, **103**, 9035–9044.

Cummins, K. L., and M. J. Murphy, 2009: An overview of lightning locating systems: History, techniques, and data uses, with an in-depth look at the U.S. NLDN. *IEEE Trans. Electromagn. Compat.*, **51**, 499–518.

Fierro, A. O., X.-M. Shao, T. Hamlin, J. M. Reisner, and J. Harlin, 2011: Evolution of eyewall convective events as indicated by intracloud and cloud-to-ground lightning activity during the rapid intensification of Hurricanes Rita and Katrina. *Mon. Wea. Rev.*, **139**, 1492–1504.

Krehbiel, P. R., 1981: *An analysis of the electric field change produced by lightning*. Ph.D. Thesis, University of Manchester Institute of Science and Technology.

Krehbiel, P. R., 1986: The electrical structure of thunderstorms. *The Earth's Electrical Environment*. National Academies Press, Washington, D.C., 90–113.

Lang, T. J., L. J. Miller, M. Weisman, S. A. Rutledge, L. J. Barker III, V. N. Bringi, V. Chandrasekar, A. Detwiler, N. Doesken, J. Helsdon, C. Knight, P. Krehbiel, W. A. Lyons, D. MacGorman, E. Rasmussen, W. Rison, W. D. Rust, and R. J. Thomas, 2004a: The Severe Thunderstorm Electrification and Precipitation Study. *Bull. Amer. Meteor. Soc.*, **85**, 1107–1126.

Lang, T. J., S. A. Rutledge, and K. C. Wiens, 2004b: Origins of positive cloud-to-ground lightning flashes in the stratiform region of a mesoscale convective system. *Geophys. Res. Lett.*, **31**, L10105, doi:10.1029/2004GL019823.

Levin, Z., Y. Yair, and B. Ziv, 1996: Positive cloud-to-ground flashes and wind shear in Tel-Aviv thunderstorms. *Geophys. Res. Lett.*, **23**, 2231–2234.

MacGorman, D. R., and W. D. Rust, 1998: *The Electrical Nature of Storms*. Oxford University Press, 422 pp.

MacGorman, D. R., W. D. Rust, P. Krehbiel, W. Rison, E. Bruning, and K. Wiens, 2005: The electrical structure of two supercell storms during STEPS. *Mon. Wea. Rev.*, **133**, 2583–2607.

Mecikalski, R. M., A. L. Bain, and L. D. Carey, 2015: Radar and lightning observations of deep moist convection across northern Alabama during DC3: 21 May 2012. *Mon. Wea. Rev.*, **143**, 2774–2794.

Molinari, J., P. Moore, and V. Idone, 1999: Convective structure of hurricanes as revealed by lightning locations. *Mon. Wea. Rev.*, **127**, 520–534.

Nakano, F., T. Morimoto, T. Ushio, and Z. Kawasaki, 2011: Lightning distribution in typhoons observed by the TRMM/LIS. *Tenki*, **58**, 117–130 (in Japanese).

Price, C., M. Asfur, and Y. Yair, 2009: Maximum hurricane intensity preceded by increase in lightning frequency. *Nat. Geosci.*, **2**, 329–332.

Rison, W., R. J. Thomas, P. R. Krehbiel, T. Hamlin, and J. Harlin, 1999: A GPS-based three-dimensional lightning mapping system: Initial observations in central New Mexico. *Geophys. Res. Lett.*, **26**, 3573–3576.

Sakurai, N., K. Iwanami, S. Shimizu, Y. Uji, S. Suzuki, T. Maesaka, K. Shimose, P. R. Krehbiel, W. Rison, and D. Rodeheffer, 2021: 3D total lightning observation network in Tokyo metropolitan area (Tokyo LMA). *J. Disaster Res.*, **16**, 778–785.

Samsury, C. E., and R. E. Orville, 1994: Cloud-to-ground lightning in tropical cyclones: A study of Hurricanes Hugo (1989) and Jerry (1989). *Mon. Wea. Rev.*, **122**, 1887–1896.

Shao, X. M., P. R. Krehbiel, R. J. Thomas, and W. Rison, 1995: Radio interferometric observations of cloud-to-ground lightning phenomena in Florida. *J. Geophys. Res.*, **100**, 2749–2783.

Squires, K., and S. Businger, 2008: The morphology of eyewall lightning outbreaks in two category 5 hurricanes. *Mon. Wea. Rev.*, **136**, 1706–1726.

Takahashi, T., 1978: Riming electrification as a charge generation mechanism in thunderstorms. *J. Atmos. Sci.*, **35**, 1536–1548.

Thomas, J. N., N. N. Solorzano, S. A. Cummer, and R. H. Holzworth, 2010: Polarity and energetics of inner core lightning in three intense North Atlantic hurricanes. *J. Geophys. Res.*, **115**, A00E15, doi:10.1029/2009JA014777.

Thomas, R. J., P. R. Krehbiel, W. Rison, S. J. Hunyady, W. P. Winn, T. Hamlin, and J. Harlin, 2004: Accuracy of the lightning mapping array. *J. Geophys. Res.*, **109**, D14207, doi:10.1029/2004JD004549.

Wang, D., D. Zheng, T. Wu, and N. Takagi, 2021: Winter positive cloud-to-ground lightning flashes observed by LMA in Japan. *IEEJ Trans. Electr. Electron. Eng.*, **16**, 402–411.

Wu, T., D. Wang, H. Huang, and N. Takagi, 2021: The strongest negative lightning strokes in winter thunderstorms in Japan. *Geophys. Res. Lett.*, **48**, e2021GL095525, doi:10.1029/2021GL095525.

Yokoyama, C., and Y. N. Takayabu, 2008: A statistical study on rain characteristics of tropical cyclones using TRMM satellite data. *Mon. Wea. Rev.*, **136**, 3848–3862.

Yoshida, S., E. Yoshikawa, T. Adachi, K. Kusunoki, S. Hayashi, and H. Inoue, 2019: Three-dimensional radio images of winter lightning in Japan and characteristics of associated charge structure. *IEEJ Trans. Electr. Electron. Eng.*, **14**, 175–184.

Zhang, W., Y. Zhang, D. Zheng, and X. Zhou, 2012: Lightning distribution and eyewall outbreaks in tropical cyclones during landfall. *Mon. Wea. Rev.*, **140**, 3573–3586.

Zheng, D., D. Wang, Y. Zhang, T. Wu, and N. Takagi, 2019: Charge regions indicated by LMA lightning flashes in Hokuriku's winter thunderstorms. *J. Geophys. Res.*, **124**, 7179–7206.